

The Impacts of Physical Layer Parameters on the Connectivity of Ad-Hoc Networks

Javad Kazemitabar Hodayoun Yousefi'zadeh Hamid Jafarkhani

Department of EECS

University of California, Irvine

[skazemit,hyousefi,hamidj]@uci.edu

Abstract— We study the effects of physical layer parameters on the connectivity of fading wireless ad-hoc networks. Relying on a symbol error rate connectivity metric for wireless ad-hoc networks, we assume a pair of nodes are connected if their bi-directional measure of connectivity satisfies a given threshold. We investigate the effects of three parameters on the connectivity phenomenon. First and assuming the nodes are distributed over a fixed finite area, we study the effects of the changes in nodes density on connectivity. Next, we measure the connectivity effects of the interference coefficients, i.e., the portion of power an interfering node contributes to other links. Finally, we experiment with threshold of link quality for connectedness. For each parameter, we also provide an intuitive explanation of the phenomena occurring in our experiments. Our simulation results show that (1) depending on the value of interference coefficient, an increase in node density may increase or decrease, and (2) increasing the interference coefficients and thresholds of link quality will decrease the connectivity of fading ad-hoc networks.

Index Terms— Ad-Hoc Networks, Rayleigh Fading Channel, Symbol Error Rate, Connectivity, Node Density, Interference, Link Quality.

I. INTRODUCTION

Wireless networks allow for establishing communication paths between different users regardless of their position. Not requiring any fixed infrastructure has made the deployment of wireless ad-hoc networks more attractive than cellular ad-hoc networks from an economical standpoint and in the context of special applications such as tactical applications. In spite of having several advantages compared to wired networks, both cellular and ad-hoc wireless networks have encountered major challenges due to requiring to transmit data over the air medium.

Investigating the connectivity of radio networks dates back to almost half a century ago. Relying on the geometric disk model and percolation theory, Gilbert [8] studied the connectivity of infinite random networks. In the geometric disk model, a random topology network is represented by a disk graph in which two nodes are considered directly connected if their distance is smaller than a given transmission radius. In the context of ad-hoc network connectivity, percolation theory [12], [9] revolves around finding conditions under which a mobile node belongs to an unbounded cluster of connected mobile nodes. Gilbert showed that there exists a critical threshold representing the minimum number of nodes within a transmission range above which a random graph is almost surely connected. He

also introduced upper and lower bounds on the critical threshold of connectivity.

Recently, the connectivity subject has received much attention due to the deployment of wireless ad-hoc networks. Some of the recent follow-on studies about the connectivity of infinite random networks relying on the geometric disk model include the work of Booth et al. [4], Philips et al. [14], and Quintanilla et al. [15]. In addition, there are a large number of articles in the context of connectivity of ad-hoc networks with a finite number of mobile nodes. Some of the related articles in this area include the work of Cheng et al. [5], Santi et al. [16], Bettstetter [3], and Dousse et al. [6].

Since geometric disk model does not capture the reality of wireless networks, Gupta et al. [10] introduced another connectivity metric based on the concept of Signal-to-Interference-Noise Ratio (SINR). According to the SINR metric, two nodes in a random topology are directly connected if their minimum SINR is greater than a given threshold. Baccelli et al. [2] utilized the SINR metric under Poisson assumptions in the context of infinite CDMA networks. Relying on the same metric, Dousse et al. [7] showed that if both node density per unit area and SINR are sufficiently high, the resulting infinite graph of an ad-hoc network is almost surely connected. Interestingly, connectivity in random networks represented by graphs of mixed short and long edges can also be related to small world networks [19].

In [11] and [20], we argued that even the SINR metric falls short of truly capturing the connectivity phenomenon in wireless ad-hoc networks. We introduced a pair of probabilistic connectivity measures based on the capacity and symbol error rates of wireless Multiple-Input Multiple-Output (MIMO) links. We related the quantities of interest to the characteristics of the physical layer such as modulation, number of antennas, and SINR. Utilizing the size of the largest connected cluster of an ad-hoc network, we focused on its connectivity.

In our studies, we noticed that the physical layer issues play a crucial role in identifying the size of the largest cluster of an ad-hoc network. For example, sending data over an open shared transmission medium causes interference resulting in degradation of link quality and connectivity. Due to the same reason, the physical location of the nodes becomes important which brings the notion of density in mind. As such, we identified the need for performing an independent study with the goal of inspecting the effects of physical layer issues on the connectivity phenomenon. This paper addresses the latter need.

In this paper, we consider the effects of physical layer parameters of the network on connectivity based on the ergodic SER measure of connectivity introduced in [20]. As the first parame-

ter of our discussion, we investigate the effects of node density changes on the connectivity of a number of nodes distributed over a fixed finite area. Next and as the second parameter, we investigate the effects of the interference coefficient capturing the shadowing gain. The third parameter of our discussion is the threshold of quality in terms of symbol error rates required for a pair of nodes to be considered directly connected.

This paper is organized as follows. In section II, we provide a review and an analysis of the utilized connectivity metric, i.e. the ergodic SER metric of [20]. Section III presents the results of our study in measuring the effects of different parameters of the physical layer on connectivity and the trade off between them. We also provide some insight when justifying our results. Finally, Section IV concludes this paper.

II. ERGODIC SER METRIC OF CONNECTIVITY

In this section, we provide a review of the connectivity metric utilized in our study. Consider an ad-hoc topology with q wireless flat fading links $\{\mathcal{L}_1, \dots, \mathcal{L}_q\}$ on which transmission powers are $\{P_1, \dots, P_q\}$, respectively. Link i is associated with the i -th transmitter/receiver pair. Each link may be connecting multiple antenna mobile nodes. Suppose, per symbol transmission power P_i is equally distributed among M_i transmit antennas of link i . The number of receive antennas for link i is assumed to be N_i . Let us assume that the $N_i \times M_j$ matrix H_{ij} represents the fading channel between the transmitter of link j and the receiver of link i . Denoting \mathbf{S}_i as the $M_i \times T$ symbol matrix of link i transmitted over discrete time blocks of length T , the received symbol matrix at link i is the following $N_i \times T$ matrix

$$\mathbf{R}_i = H_{ii}\mathbf{S}_i + \sum_{j \neq i} H_{ij}\mathbf{S}_j + \mathbf{n}_i \quad (1)$$

where the channel matrices H_{ij} consist of complex Gaussian random variable elements. Associated with each element $H_{ij}(n, m)$ of channel matrices, we define the fading factors $F_{ij}(n, m) = |H_{ij}(n, m)|^2$. For each link i , the SER can be derived as an exact function of the average SINR and the corresponding fading factors $F_{ii}(n, m)$.

Denoting G_{ij} as the scalar shadowing (path) gain in the absence of fading from the transmitter of link j to the receiver of link i , the signal-to-interference-noise ratio for link i is defined as

$$SINR_i = \frac{G_{ii} \frac{P_i}{M_i} \sum_{m=1}^{M_i} \sum_{n=1}^{N_i} F_{ii}^{(m,n)}}{\sum_{j \neq i} G_{ij} \frac{P_j}{M_j} \sum_{m=1}^{M_j} \sum_{n=1}^{N_i} F_{ij}^{(m,n)} + N_i P_i^{(n)}} \quad (2)$$

where the numerator term indicates the desired received power at the receiver of link i , and the numerator terms indicate the power of interference and noise signals. We note that the power of white Gaussian noise $P_i^{(n)}$ on link i is multiplied by N_i .

In [21], we identify the expressions of SER for link i in terms of the number of signal points in the constellation L_i and the average signal-to-interference-noise ratio $SINR_i$. Our calculations are carried out under the assumption of facing a complex Gaussian noise signal and utilizing Phase Shift Keying (PSK) modulation.

TABLE I

THE VALUES OF β FOR DIFFERENT ANTENNA CONFIGURATIONS OF INTEREST.

	1×1	2×1	1×2	2×2
β	1	0.5	1	0.5

Based on our analysis, the symbol error rate of link i utilizing BPSK modulation can be derived as

$$SER_i = Q\left(\sqrt{2\beta\Upsilon_i \overline{SINR}_i}\right) \quad (3)$$

where \overline{SINR}_i is the average signal-to-interference-noise-ratio of link i calculated by taking the expected value of Equation (2) and Υ_i is defined as

$$\Upsilon_i = \sum_{m=1}^{M_i} \sum_{n=1}^{N_i} F_{ii}(n, m) \quad (4)$$

Further, β is a constant that depends on the antenna configuration. The values of β for the configurations of interest are shown in Table I. Similar expressions can be given in the case of utilizing L-PSK modulation.

Based on the assumption of facing a flat Rayleigh channel and in the duration of a frame, the channel matrices $H_{ij}(n, m)$ consist of Gaussian random variables while the shadowing gains G_{ij} and transmission powers P_i are constant. Since $H_{ij}(n, m)$ are random variables and $F_{ij}(n, m) = |H_{ij}(n, m)|^2$, the fading factors $F_{ij}(n, m)$ are themselves random variables. Similarly, $SINR_i$ and SER_i as defined in Equation (2) and (3) are also random variables. However the expectation \overline{SINR}_i is not a random variable. Rather, it represents a probabilistic average. In order to express our connectivity criterion, we are interested in determining the distribution of the random variables SER_i .

When the channel matrix is identified by complex Gaussian noise elements, $|H_{ij}|$ has a marginal Rayleigh density function [13] in the form of

$$p_H(|H_{ij}|) = \frac{|H_{ij}| e^{-|H_{ij}|^2/2\mu_{ij}^2}}{\mu_{ij}^2} \quad (5)$$

where μ_{ij}^2 equals to half of the average power of all of the multipath components affecting the link.

We now express two properties of random variables [13].

- **Property 1:** If x and y are random variables satisfying $y = g(x)$, then the PDF of y satisfies $f_y(y) = \frac{f_x(x_1)}{g'(x_1)} + \dots + \frac{f_x(x_q)}{g'(x_q)}$ where x_1, \dots, x_q are the real roots of $y = g(x)$ and $g'(x)$ represents the derivative of $g(x)$ with respect to x .
- **Property 2:** If the PDF set $\{f_{x_1}(x_1), \dots, f_{x_q}(x_q)\}$ is associated with the set of independent random variables $\{x_1, \dots, x_q\}$, then the PDF of their sum $z = x_1 + \dots + x_q$ is calculated as $f_z(z) = f_{x_1}(z) * \dots * f_{x_q}(z)$ where $*$ represents the convolution operator.

Based on the first property above, the PDF of F_{ii} can be expressed as

$$p_F(F_{ii}) = \frac{1}{2\sqrt{F_{ii}}} p_H(\sqrt{F_{ii}}) \quad (6)$$

Once the PDFs of F_{ii} terms are calculated and assuming they are spatially uncorrelated, the second property above can be utilized to specify the PDF of Υ_i as defined in Equation (4). Finally, the PDF of $SE R_i$ as defined in Equation (3) can be calculated in terms of the PDF of the random variables Υ_i relying on the the first property above.

Having specified the PDF of $SE R_i$, we assume that the fading wireless channel is ergodic. Under the assumption of facing an ergodic Rayleigh channel and utilizing L-PSK modulation, the average value $\overline{SE R}_i$ can be specified by calculating the expected value of Equation (3) as

$$\overline{SE R}_i = \int_0^\infty \left(\frac{1}{\pi} \int_0^{(L_i-1)\pi/L_i} \exp\left(-\frac{2\beta \Upsilon_i \overline{SINR}_i}{2 \sin^2 \tau}\right) d\tau \right) p_\Upsilon(\Upsilon_i) d\Upsilon_i \quad (7)$$

where $p_\Upsilon(\cdot)$ is the Probability Density Function (PDF) of the random variable Υ_i . In [21], we calculate closed-form expressions of the integral of (7) in terms of the number of signal points in the constellation L_i and the average signal-to-noise ratio \overline{SINR}_i . In what follows, we provide a brief review of our discussion considering the fact that in the current discussion the quantity of interest is \overline{SINR}_i rather than \overline{SNR}_i . First, we introduce the symbol error rate of a $1 \times N_i$ link using Maximum Ratio Combining (MRC) as

$$\overline{SE R}_i = \frac{L_i-1}{L_i} - \frac{1}{\pi} \sqrt{\frac{\vartheta_i}{1+\vartheta_i}} \left\{ \left(\frac{\pi}{2} + \tan^{-1} \theta_i \right) \sum_{j=0}^{N_i-1} \binom{2j}{j} \frac{1}{[4(1+\vartheta_i)]^j} + \sin(\tan^{-1} \theta_i) \sum_{j=1}^{N_i-1} \sum_{k=1}^j \frac{\zeta_{kj}}{(1+\vartheta_i)^j} \times [\cos(\tan^{-1} \theta_i)]^{2(j-k)+1} \right\} \quad (8)$$

where $\vartheta_i = \overline{SINR}_i \sin^2(\frac{\pi}{L_i})$, $\theta_i = \sqrt{\frac{\vartheta_i}{1+\vartheta_i}} \cot \frac{\pi}{L_i}$, and $\zeta_{kj} = [\binom{2j}{j}] / [\binom{2(j-k)}{j-k}] 4^i [2(j-k)+1]$.

Noting that the number of bits per symbol is related to the number of signal points in the constellation L_i as $\log_2 L_i$, the result of Equation (8) for a 1×4 link utilizing BPSK modulation with $L_i = 2$ is expressed as

$$\overline{SE R}_i = \frac{1}{2} - \frac{1}{2} \sqrt{\frac{\overline{SINR}_i}{1+\overline{SINR}_i}} \left(\sum_{j=0}^3 \binom{2j}{j} \frac{1}{[4(1+\overline{SINR}_i)]^j} \right) \quad (9)$$

Next, we focus on the symbol error rates of multiple transmit antenna links using Space-Time Block Codes (STBCs) of [1] and [18]. We note that in the case of STBCs and under the assumption of a fixed amount of power available at the transmitter, the power is split equally between the transmit antennas of each link in a given symbol interval. On the contrary and in the case of an MRC link, only one symbol is transmitted in each symbol interval and the total power is allocated to it. Since the product of transmit and receive antennas specifies the diversity gain, different configurations of antennas utilizing either MRC or STBC can yield similar diversity gains. For example, the diversity gain of a 1×4 MRC link is the same of that of a 2×2 STBC link. As such, the symbol error rate expression of a 1×4 MRC link can be used to specify the symbol error rates of a

2×2 STBC for as long as the effects of transmission power are properly captured. We capture the transmission power split effect in terms of \overline{SINR}_i . We derive the symbol error rate of a 2×2 STBC link by replacing \overline{SINR}_i with $\frac{\overline{SINR}_i}{2}$ in Equation (8). With the choice of BPSK modulation, the result for a 2×2 link is expressed as

$$\overline{SE R}_i = \frac{1}{2} - \frac{1}{2} \sqrt{\frac{\overline{SINR}_i}{2+\overline{SINR}_i}} \left(\sum_{j=0}^3 \frac{\binom{2j}{j}}{[2(2+\overline{SINR}_i)]^j} \right) \quad (10)$$

Based on the ergodic symbol error rates of a MIMO link, we express our ergodic connectivity metric in the form of

$$\overline{SE R}_i \leq S_{out} \quad (11)$$

where S_{out} is the threshold of connectivity.

III. EXPERIMENTAL RESULTS

As indicated in the previous section, the ergodic connectivity metric of (11) is expressed in terms of the parameters of the physical layer. The latter includes the number of antennas, modulation, SINR, and the threshold of connectivity. In this section, we investigate the effects of physical layer parameters on the normalized size of the largest connected cluster in an ad-hoc network. We note that a fully connected ad-hoc network is represented by a normalized cluster size of 1.

Before proceeding with the explanation of our experiments, we further note that we are investigating the connectivity of wireless ad-hoc networks accommodating mobile nodes equipped with two antennas. While the mobile nodes utilize STBCs of [1] and [18] when transmitting, they rely on MRC when receiving. In addition, we assume that the slow fading wireless channel characterized by a Rayleigh distribution is quasi-static and flat implying that the shadowing gains are constant over a frame but vary independently from one frame to another.

The following describes the general settings of our experiments. We consider a set of nodes distributed on a 2-D domain with an area of 1000 square meters according to a Poisson point process. All of the nodes are utilizing BPSK modulation. The shadowing gains for each link are computed as $G_{ii} = \frac{1}{d_{ii}^\alpha}$ and $G_{ij} = \frac{\eta}{d_{ij}^\alpha}$ for $i \neq j$, where d_{ij} represents propagation path length from the transmitter of link j to the receiver of link i . The factor η can be viewed as the common power falloff with frequency in an FDMA system, or the spreading gain in a CDMA system. We assume that each node utilizes a total transmission power of $P = 1W$ on the combined set of its outgoing links with the total transmission power split equally between the transmit antennas. The expected value of the noise power on each path is assumed to be $10\mu W$. A pair of nodes are considered to form a link L_i if the connectivity metric of (11) holds. We note that link connectivity may be directional implying that a first node can transmit to a second node while the second node may not be able to transmit to the first node. In our experiments, we consider link connectivity exists if both nodes can transmit and receive from one another under the connectivity criterion.

For the random topology described above, we consider three sets of experimentation scenarios. In the first scenario, we consider a fixed connectivity threshold S_{out} in a network with 200

nodes and study the effects of interference by choosing different values for η . In the second experimentation scenario, we consider the effects of variations in the threshold of connectivity S_{out} while keeping the rest of the parameters fixed. In the third experimentation scenario, we investigate the effects of variations in the node density for different values of η . In each of the experiments corresponding to these scenarios, we find the largest connected cluster of the network and find its normalized size.

Fig. 1 provides the results of our first set of experiments. It depicts the normalized size of the largest connected cluster versus the interference coefficient η . The figure has a variation range of $[5e-8, 1]$ for η while keeping the other parameters fixed. The curve shows that increasing the value of η from $5e-8$ to 0.04 yields a sharp drop in the normalized size of the largest connected cluster from 1 to about 0.01. Passed the knee of the curve, the connectivity is almost non-existent for the ad-hoc network of our study.

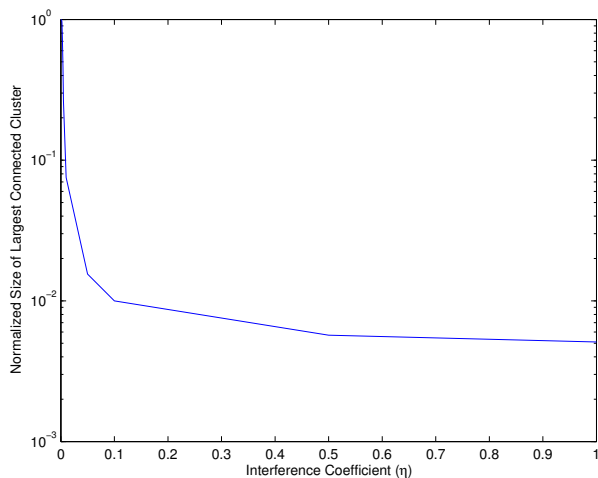


Fig. 1. The drawing of the normalized size of the largest connected cluster versus the interference coefficient η for a connectivity threshold of $S_{out} = 0.001$.

Fig. 2 shows the connectivity graphs of three points before, on, and after the knee of the drawing of Fig. 1. We observe that increasing the interference coefficient will decrease connectivity and justify our observation based on the following argument. Since a higher interference coefficient represents a lower SINR, the symbol error rate increases and a smaller number of links can satisfy the connectivity criterion.

Fig. 3 shows the effects of variations in the connectivity threshold S_{out} on the normalized size of the largest connected cluster, i.e., the minimum symbol error rate required for connectivity. Reviewing the curve, we observe that tightening the connectivity threshold while keeping all other parameters fixed will decrease connectivity. This is expected, because applying a tighter threshold allows for a lower number of links to satisfy the connectivity criterion.

Fig. 4 and 5 show the effects of variations of node density on connectivity for two different choices of the interference coefficient η . Interestingly, the effects of node density variations impact connectivity in conjunction with the interference coef-

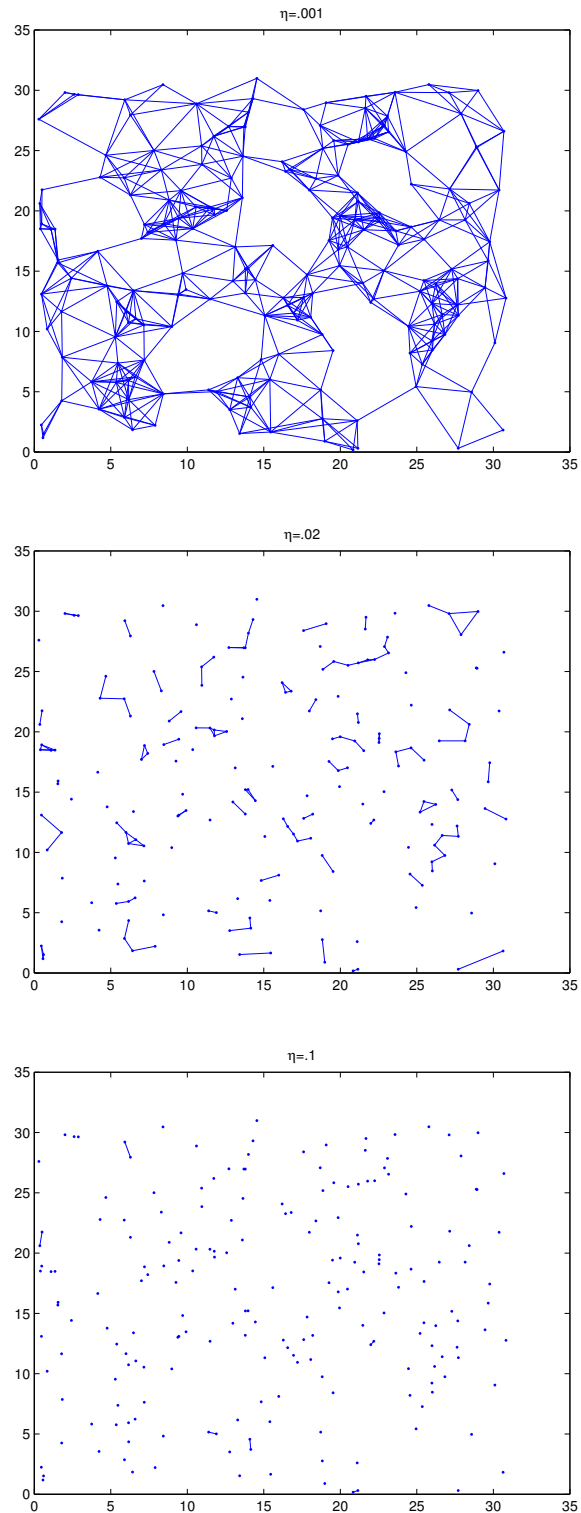


Fig. 2. Connectivity graphs associated with three points before, on, and after the knee of the drawing of Fig. 1.

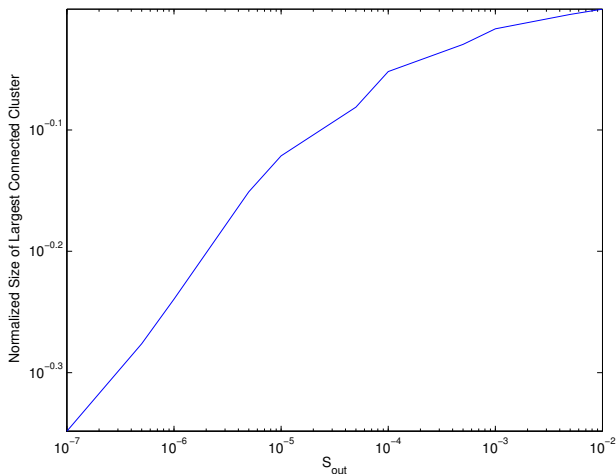


Fig. 3. The drawing of the normalized size of the largest connected cluster versus the threshold of connectivity S_{out} for an interference coefficient $\eta = 0.002$.

ficient η . As it can be seen in Fig. 4, increasing node density with a large interference coefficient η will lead to a decrease in the connectivity profile. On the contrary, Fig. 5 shows that increasing node density in conjunction with a small value of η , improves the connectivity profile. This result is in agreement

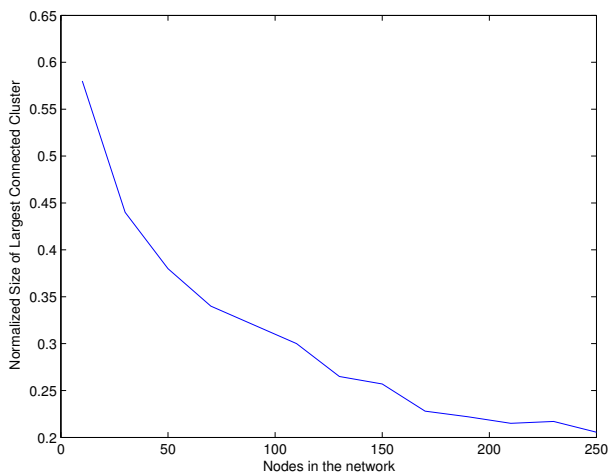


Fig. 4. The drawing of the normalized size of the largest connected cluster versus the number of nodes with connectivity threshold of $S_{out} = 0.001$ and $\eta = 0.001$. For this choice of η , connectivity degrades with increasing the number of nodes in the network.

with the work of [6], where in the form of a theorem, the possibility of percolation for infinite networks was explained under different interference profiles. The reason behind these consistent observations is that an increase in node density will impact the effects of two contradicting factors. When nodes become closer, the distance between neighboring nodes will decrease which leads to a lower path loss and higher received power. On the other hand, a decrease in distance or an increase in node density will increase the amount of interference caused by interfering nodes. The choice of dominant factor among these

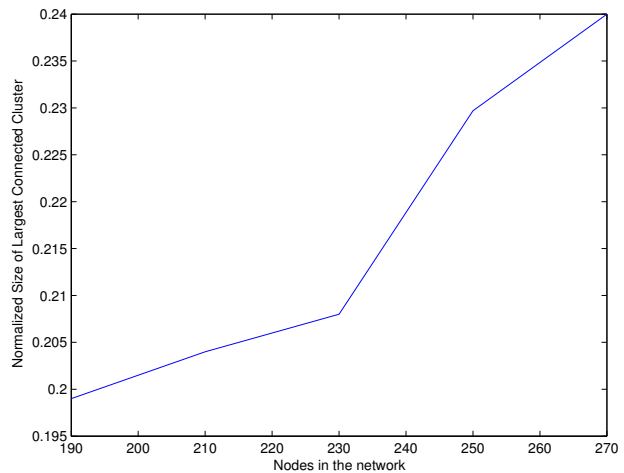


Fig. 5. The drawing of the normalized size of the largest connected cluster versus the number of nodes with connectivity threshold of $S_{out} = 1e-6$ and $\eta = 1e-5$. For this choice of η , connectivity improves with increasing the number of nodes in the network.

two will then depend on the interference coefficient η . As it is shown in Fig. 4, for the case of $\eta = 0.001$ the second factor was dominant and the connectivity kept decreasing with the increase of node density. However for the case of $\eta = 1e-5$, the first factor is dominant and an increase in node density results in an increase in the size of the largest connected cluster.

IV. CONCLUSION

In this paper we investigated the effects of variations of the physical layer parameters on the connectivity of fading wireless ad-hoc networks. We assumed a pair of nodes are connected if their bi-directional measure of connectivity, i.e., their ergodic symbol error rate falls below a given threshold. We focused on a set of experiments pertaining to the following factors. First, we looked at the effects of variations of node density in a fixed finite area. Second, we studied the effects of interference coefficient or the portion of power an interfering node contributes to other links. Finally, we studied the effects of changing the threshold of link quality for connectedness. For each parameter, we also provided an intuitive explanation of the phenomenon occurring in our experiments. Our experimentation results showed that (1) depending on the value of interference coefficient, an increase in the node density may increase or decrease connectivity, and (2) increasing the interference coefficient and the threshold of link quality will decrease connectivity.

REFERENCES

- [1] S.M. Alamouti, "A Simple Transmitter Diversity Scheme for Wireless Communications," IEEE JSAC, November 1998.
- [2] F. Baccelli, B. Blaszczyzyn, "On A Coverage Process Ranging from the Boolean Model to the Poisson Voronoi Tessellation, with Applications to Wireless Communications," Advance Applied Probability, vol. 33(2), 2001.
- [3] C. Bettstetter, "On the Minimum Node Degree and Connectivity of a Wireless Multihop Network," In Proc. ACM MOBIHOC, 2002.
- [4] L. Booth, J. Bruck, M. Franschetti, R. Meester, "Continuum Percolation and the Geometry of Wireless Networks," Annals of Applied Probability, 2002.

- [5] Y.-C. Cheng, T. G. Robertazzi, "Critical Connectivity Phenomena in Multihop Radio Models," *IEEE Trans. Communications*, July 1989.
- [6] O. Dousse, P. Thiran, M. Hasler, "Connectivity in Ad-Hoc and Hybrid Networks," In Proc. IEEE INFOCOM, 2002.
- [7] O. Dousse, F. Baccelli, P. Thiran, "Impact of Interferences on Connectivity in Ad-Hoc and Networks," In Proc. IEEE INFOCOM, 2003.
- [8] E. N. Gilbert, "Random Plane Networks," *SIAM J.*, vol. 9, pp. 533-543, 1961.
- [9] G. Grimmett, "Percolation, 2nd Edition," Springer, ISBN 3540649026, 1999.
- [10] P. Gupta, P. R. Kumar, "Critical Power for Asymptotic Connectivity in Wireless Networks," *Stochastic Analysis, Control, Optimization and Applications: A Volume in Honor of W.H. Fleming, 1998*, edited by W.M. McEneaney, G. Yin, and Q. Zhang, (Eds.) Birkhauser.
- [11] H. Jafarkhani, H. Yousefi'zadeh, J. Kazemitabar, "Capacity-Based Connectivity of MIMO Fading Ad-Hoc Networks," To Appear In Proc. IEEE GLOBECOM 2005.
- [12] R. Meester, R. Roy, "Continuum Percolation," Cambridge University Press, ISBN 052147504, 1996.
- [13] A. Papoulis, S.U. Pillai, "Probability, Random Variables, and Stochastic Processes, Fourth Edition," McGraw-Hill, ISBN 0071122567, 2002.
- [14] T.K. Philips, S.S. Panwar, A.N. Tantawi, "Connectivity Properties of a Packet Radio Network Model," *IEEE Trans. Information Theory*, September 1989.
- [15] S. Quintanilla, S. Torquato, R.M. Ziff, "Efficient Measurements of the Percolation Threshold for the Fully Penetrable Disks," *Journal of Physics*, October 2000.
- [16] P. Santi, D.M. Blough, "An Evaluation of Connectivity in Mobile Wireless Ad Hoc Networks," In Proc. IEEE DSN, 2002.
- [17] V. Tarokh, H. Jafarkhani, A.R. Calderbank, "Space-Time Block Coding for Wireless Communications: Performance Results," *IEEE JSAC*, March 1999.
- [18] V. Tarokh, H. Jafarkhani, A.R. Calderbank, "Space-Time Block Coding from Orthogonal Designs," *IEEE Trans. Information Theory*, July 1999.
- [19] D. Watts, S. Strogatz, "Collective Dynamics of Small-World Networks," *Nature*, June 1998.
- [20] H. Yousefi'zadeh, H. Jafarkhani, J. Kazemitabar, "Outage Probability Metrics of Connectivity for MIMO Fading Ad-Hoc Networks," Submitted to *IEEE Trans. Mobile Computing*, Available at <http://newport.eecs.uci.edu/~hyousefi/publ/connTMC.pdf>.
- [21] H. Yousefi'zadeh, H. Jafarkhani, M. Moshfeghi, "Power Optimization of Wireless Media Systems with Space-Time Block Codes," *IEEE Trans. Image Processing*, July 2004.